AIP | Applied Physics Letters

Experimental surface-enhanced Raman scattering response of two-dimensional finite arrays of gold nanopatches

M. Grande, G. V. Bianco, M. A. Vincenti, T. Stomeo, D. de Ceglia et al.

Citation: Appl. Phys. Lett. **101**, 111606 (2012); doi: 10.1063/1.4752719
View online: http://dx.doi.org/10.1063/1.4752719
View Table of Contents: http://apl.aip.org/resource/1/APPLAB/v101/i11
Published by the American Institute of Physics.

Experimental surface-enhanced Raman scattering response of two-dimensional finite arrays of gold nanopatches

M. Grande,[1,a),b)] G. V. Bianco,[2,a),c)] M. A. Vincenti,[3] T. Stomeo,[4] D. de Ceglia,[3] M. De Vittorio,[4,5] V. Petruzzelli,[1] M. Scalora,[6] G. Bruno,[2] and A. D'Orazio[1]
[1]*Dipartimento di Elettrotecnica ed Elettronica, Politecnico di Bari, Via Re David 200, 70125 Bari, Italy*
[2]*Inorganic Methodologies and of Plasmas, IMIP-CNR, via Orabona 4, 70126 Bari, Italy*
[3]*AEgis Technologies Inc., 410 Jan Davis Dr., Huntsville 35898-5000, Alabama, USA*
[4]*Italian Institute of Technology (IIT), Center for Bio-Molecular Nanotechnology, Via Barsanti, Arnesano, Lecce 73010, Italy*
[5]*National Nanotechnology Laboratory (NNL), CNR-ISTITUTO DI NANOSCIENZE, Dip. Ingegneria dell'Innovazione, Università Del Salento, Via Arnesano, 73100 Lecce, Italy*
[6]*Charles M. Bowden Research Center, RDECOM, Redstone Arsenal, Alabama 35898-5000, USA*

(Received 28 May 2012; accepted 30 August 2012; published online 14 September 2012)

We experimentally investigate the nonlinear response of two-dimensional periodic arrays composed of gold nanopatches on silicon substrate, functionalized by means of a conjugated rigid thiol. The surface-enhanced Raman scattering (SERS) response is empirically evaluated using a laser source operating in the visible spectral range at $\lambda = 633$ nm. Nonlinear results are then correlated to optical and structural properties of the samples under investigation. SERS mapping and estimation of the SERS enhancement factor are examined to determine stability and reproducibility of the results, highlighting also the contribution of the plasmonic resonance excited in the two-dimensional periodic array, and the dependence on the numerical aperture of the microscope objective used in the micro-Raman system. © *2012 American Institute of Physics*. [http://dx.doi.org/10.1063/1.4752719]

Surface-enhanced Raman scattering (SERS) is a Raman spectroscopic (RS) technique aimed at enhancing Raman signals that result from the interaction between molecules and metal surfaces or nanoparticles.[1] This technique provides detailed information on the composition and the chemical structure of single molecules or compounds in a non-destructive and non-invasive way. SERS spectroscopy has experienced fast growth during the last few decades since it was recognized as a powerful tool in many research areas such as chemistry, surface science, spectroscopy, biomedicine, cancer, and toxin detection. Therefore, there is significant interest in designing and optimizing SERS-oriented substrates. It is worth noting that noble metal nanoparticles have played an important role in the realization of SERS substrates thanks to their resonances due to the excitation of surface plasmon polaritons (SPPs) and localized surface plasmons (LSPs).[2,3] A wide class of SERS substrates based on colloidal and sputtered nanoparticles have been proposed.[4–8] However, colloidal stability cannot be predicted or controlled due to colloidal aggregation phenomena, and even if roughened surfaces were employed, the standardization and reproducibility of the roughening are not straightforward.[4] Moreover, SERS enhancement arising from sputtered nanostructures is not easily reproducible since it depends on geometrical parameters such as shape and size, which are often difficult to control and replicate.[8] Additionally, in some cases, the realization of particular spatial distributions on the substrate turns out to be tough, especially when the nanostructures must be placed close one to each other in order to achieve intense field hotspots. All these aspects reveal and highlight the limitations of these nanostructures, which do not allow full control of the quality of SERS substrates.

An effective way to overcome limitations introduced by such random structures is to employ periodic arrangements by means of fabrication protocols based on electron beam lithography (EBL) or nano-imprinting litography (NIL). These technologies allow the realization of nanostructures with very-high control and reproducibility. To date, different solutions have been proposed, such as arrays of nanocavities, nanodisks, nanoholes, and double-nanoholes.[9–13]

In this paper, we report on the surface-enhanced Raman scattering response of a two-dimensional periodic array of gold nano-patches functionalized by means of a conjugated, rigid thiol on silicon substrate (Fig. 1). These structures can support three different resonances: (a) a narrow band resonant state involving the whole grating; (b) a leaky mode due to the coupling between a SPP and the impinging light; and (c) a broadband Fabry-Perot (FP)-like resonance due to the transverse-electro-magnetic (TEM) guided mode generated in the slit, which acts as a metal-insulator-metal (MIM) waveguide.[14,15] In contrast, periodic arrays based on nanoholes cannot support FP resonances since the presence of a single conductor forbids the coupling of TEM-like modes.[14] Therefore, the presence of this resonance introduces a degree of freedom in the optimization of the plasmonic response of the two-dimensional (2D) arrays.[16] Moreover, two-dimensional periodic arrays offer another advantage with respect to nanoparticles since they are insensitive to incident polarization when a square unit cell is adopted.[17] This feature makes this device particularly attractive because a careful source-sample alignment is not required.

[a)]M. Grande and G. V. Bianco equally contributed to the work.
[b)]Electronic mail: grande@deemail.poliba.it.
[c)]Electronic mail: giuseppevalerio.bianco@cnr.it.

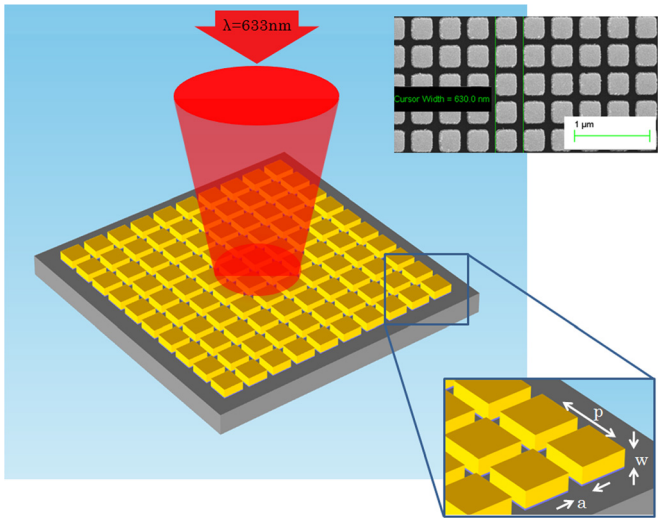

FIG. 1. Sketch of the functionalized 2D gold patch array. Inset: scanning electron microscope image of the fabricated device.

Metal arrays can be designed for a specific working wavelength by choosing properly geometrical properties such as the periodicity p, the slit aperture a, and the metal thickness w (Fig. 1). An extensive description of the linear properties of these structures was carried out elsewhere.[18,19] In order to set the working wavelength at $\lambda = 633$ nm, we performed the experiment considering an array with periodicity $p = 630$ nm, while the slit aperture a is varied in the range 72 nm to 120 nm.

In this letter, we also compare the nonlinear response of the 2D periodic gold array with a conventional plasmonic platform consisting of a sputtered gold nanoparticle ensemble. We show the different behaviour of the two systems and highlight the dependence of the SERS signal on the numerical aperture (NA) of the micro-Raman spectrometer, the functionalization process of the gold surface. The analysis of the angular variation due to the numerical aperture is extremely important to understand the real benefits and limitations of periodic arrays in micro-Raman systems that are employed in the detection of the Raman signals where resolutions down to a few microns are required (in contrast to the macro-Raman systems where the resolution can reach values between 100 μm to and a few millimeters).

The periodic metal array was fabricated by means of an electron beam lithography step followed by thermal evaporation and lift-off processes. The 2D patterns were written using a Raith150 e-beam lithography system operating at 30 kV. A bi-layer, composed of a 500 nm-thick polymethyl methacrylate (PMMA)-MA and 200 nm-thick PMMA layers, was adopted as positive resist to ensure good resolution of e-beam writing. The 700 nm-thick resist layer insures a good mask for the evaporation of the gold layer (200 nm) by means of a thermal evaporator with a current of 300 A and a deposition rate of about 2 Å/s. Furthermore, in order to increase the adhesion of the gold on the silicon substrate, a 5 nm-thick adhesion layer of chrome is previously evaporated. Finally, the sample is immersed in an acetone bath for the lift-off process that releases the final device. The inset in Fig. 1 shows the scanning electron microscope (SEM) image of the final device. The roughness inspection of the evaporated gold layer is carried out by means of an atomic force microscope (AFM), yielding a root mean square value of about 6 nm. The final device is functionalized by means of a conjugated rigid thiol, 4-methoxy-terphenyl-4″-methanethiol (TPMT), forming a very dense, closely packed, reproducible 18 Å-thick, self-assembled monolayer (SAM).[20] The SAM formation is carried out by dipping the substrates for 1 h in 1 mM solutions of TPMT in CH_2Cl_2 at the temperature of 25 °C. Samples were subsequently rinsed with solutions solvents and dried under a N_2 stream.[20]

The fabricated sample was characterized by means of a Horiba Jobin-Yvon LabRAM HR-VIS micro-Raman spectrometer equipped with a 633 nm laser source (laser power = 20 mW) that is filtered by a neutral density filters. The thin layer of conjugated rigid thiol slightly red-shifts the plasmonic resonance (full-width half-maximum, FWHM is ~20 nm) by a few nanometers without twisting the optical response of the device.[15,18] Figure 2(a) shows an example of the Raman spectrum of the conjugated rigid thiol in the range 200 cm^{-1} to 1800 cm^{-1} when $a = 96$ nm and a NA = 0.25, respectively. Details of the Raman mode assignments are reported in Ref. 20. For completeness, the Raman spectrum of the flat gold film is also reported as reference showing that the signal is negligible. Hereinafter, our analysis will be focused on the highest intensity peak centred at 1603 cm^{-1}. Furthermore, in our approach, we improve our measurements averaging the Raman signal corresponding to 1603 cm^{-1} peak over an area of 100 μm^2 (10 × 10 measurement points) in order to minimize the non-uniformity due to the functionalization process (Figure 2(b)). This area is wide enough since it covers a region of 15 × 15 gold patches.

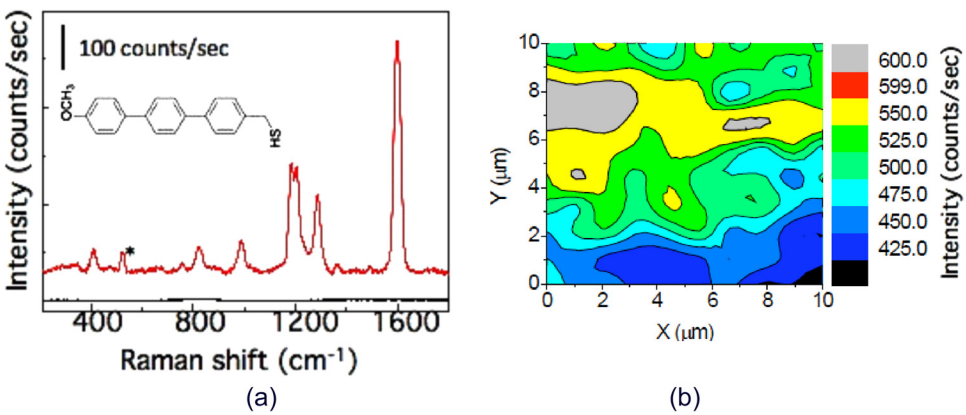

FIG. 2. (a) Raman spectra of TMTP (inset: molecule scheme) for the array with p, a, and NA equal to 630 nm, 96 nm, and 0.25, respectively (the peak with the star refers to the c-Si Raman signal). The black curve corresponds to the reference signal of the flat gold film (SERS spectrum was shifted vertically for clarity); (b) intensity map for the peak centred at 1603 cm^{-1}.

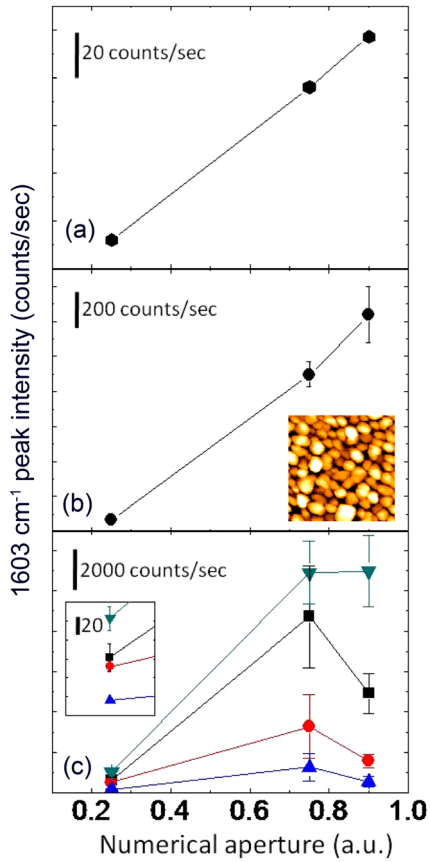

FIG. 3. Intensity of the strongest peak centred at 1603 cm^{-1} for: (a) normal Raman spectra of 1M TPMT solution in CH_2Cl_2 drop casted on c-Si substrate; (b) SERS spectra of TPMT self-assembled on sputtered gold nanoparticles (inset: AFM measurement of a 500 nm × 500 nm region revealing nanoparticles with a averaged height and diameter equal to 17 nm and 33 nm, respectively) and (c) on the 2D array of gold nanopatches for a slit aperture *a* equal to 72 nm (blue triangles), 96 nm (red dots), 108 nm (black squares), and 120 nm (green triangles), respectively. The normal Raman spectra have been acquired without the presence of the neutral filter in order to maximize the signal while a neutral filter D1 has been employed for the SERS spectra.

Figure 3 shows the intensity of the peak centred at 1603 cm^{-1} for (a) normal Raman spectra of 1 M TPMT in solution and SERS spectra of TPMT self-assembled on (b) a conventional SERS substrate based on sputtered gold nanoparticles on silicon substrate,[7] and on (c) the proposed 2D array of gold nanopatches. The plot reports three different numerical apertures NA = 0.25, 0.75, and 0.9 that correspond to a spot diameter (number of patches) equal to 3.07 μm (~5 patches), 1.02 μm (~1.6 patches), and 0.854 μm (~1.3 patches), respectively. From the plot, it can be inferred that the peak intensity in the case (c) shows a 25 - and 200-fold increase with respect to the (b) and (a) cases, respectively, when NA = 0.75 since the peak intensities are equal to about 180 422, 7241, and 907 counts/s, respectively. Moreover, the signals related to the TPMT in solution and TPMT deposited on sputtered gold nanoparticles increase monotonically with the numerical aperture. On the contrary, the nonlinear response of the 2D array shows a maximum value for the 0.75 NA. This feature reveals the superposition of two distinct phenomena: when NA increases, the angle of the incident source increases and, on the other hand, the number of the gold patches decreases. Therefore, while at higher NAs the collected signal is larger, the plasmonic resonance intensity fades because fewer patches are illuminated. This clearly shows that in periodic structures, the plasmonic resonance is the result of the collective response of the gold nanopatch ensemble, hence the resonance strength increases with the number of patches up to a limit where any addition of illuminated patches does not contribute to the resonance.[14] The data reported in Figure 2 allow us to estimate the enhancement factor (EF) when the numerical aperture is changed for several apertures:[21]

$$EF = \frac{I_{SERS}/N_{SERS}}{I_{RAMAN}/N_{RAMAN}}, \quad (1)$$

where I_{SERS}, I_{RAMAN}, N_{SERS}, and N_{RAMAN} are the SERS and Raman signal intensities and molecules numbers, respectively (Figure 3). N_{SERS} was derived as the total patch surface area irradiated by the laser divided by the TPMT SAM surface distribution density (8.0×10^{-10} mol/cm^2 from Ref. 22) while N_{RAMAN} was derived by considering the irradiated TPMT solution volume and its concentration. Moreover, N_{SERS} and N_{RAMAN} depend on the numerical aperture since the spot size, and hence the acquisition volume, is varied. We note that I_{SERS} and I_{RAMAN} were normalized by taking into account the optically neutral filter used in the measurement.

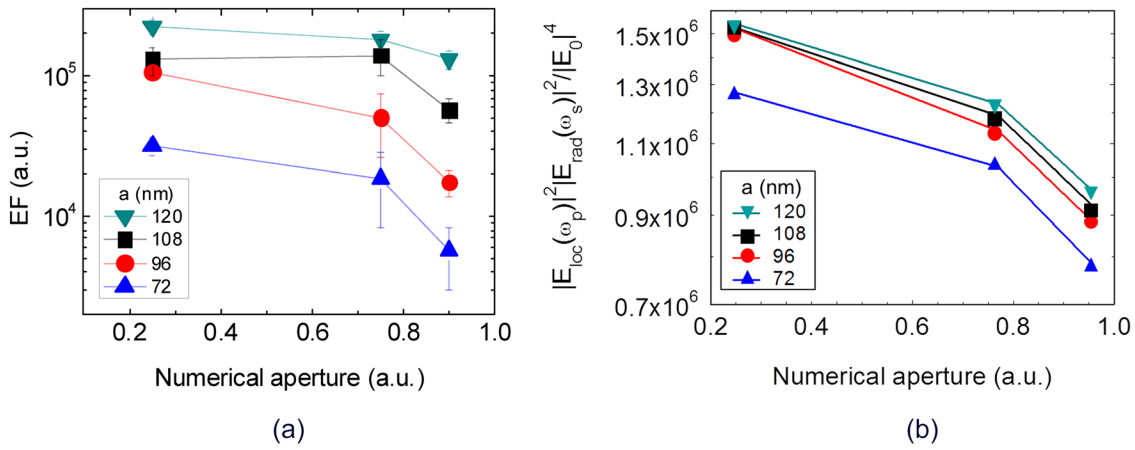

FIG. 4. (a) Experimental EF for the 2D array of gold nanopatches for several numerical apertures and (b) simulation results.

Figure 4(a) clearly proves that two-dimensional arrays show the same behaviour regardless of aperture variation. Moreover, the figure demonstrates that the Raman signal increases as the numerical aperture becomes larger in a stronger way with respect to the nanoholes structures reported in Ref. 11. This behaviour is fully consistent with a numerical analysis that shows how the absorption value, and hence field enhancement, is strictly related to the number of illuminated gold patches (Figure 4(b)). Figure 4(b) in fact reveals an almost perfect reconstruction of the trend measured for the EF obtained through the evaluation of the ratio $|E_{loc}(\omega_p)|^2\ |E_{rad}(\omega_S)|^2/|E_0|^4$, where $E_{loc}(\omega_p)$, $E_{rad}(\omega_S)$, and $E_0(\omega)$ are the pump signal, the Stokes signal, and the incident field for different Gaussian beam sizes and numerical apertures. $E_{loc}(\omega_p)$ and $E_{rad}(\omega_S)$ have been obtained by averaging the electric field over the active surface, i.e., on the gold nanotiles. We stress that we considered constant irradiance for all simulations in order to reproduce correctly the experimental results. Moreover, the simulated set up represents an additional tool to indirectly predict the maximum absorption (enhancement factor) that can be reached by the micro-Raman system in the limit where an infinite number of gold patches is illuminated.

Finally, we point out that the sputtered gold nanoparticles are not sensitive to the change of the microscope objective since the plasmonic resonance is due to the single nanoparticles (EF is equal to $\sim 10^4$). In contrast, the 2D array shows a knee where NA = 0.75, as above-mentioned, and reveals a 10-fold improvement with an EF of about 2×10^5.

In conclusion, we have reported the results of the nonlinear characterization of 2D gold nanopatches arrays on a silicon substrate and found a dramatic improvement in the Raman signal when the laser wavelength excites the surface waves of periodic nanostructures. The SERS response was empirically investigated using laser sources operating in the visible spectral range and correlated to their specific optical and structural properties. SERS mapping and estimation of the provided SERS EF were carried out revealing an EF of about 2×10^5. These values are either comparable or better than other configurations reported in literature.[9–13,23,24] The analysis of the influence of NA on the EF also revealed that for micro-Raman systems a good trade-off between the NA and the number of illuminated patches is required in order to maximize the SERS signal. Moreover, these findings clearly demonstrate that the periodicity can be designed to optimize and improve the nonlinear response of the functionalized metallic nanostructures.

The simple geometry, the insensitivity to the electric field polarization, the straightforward design, and the possibility of an effortless calculation of the number of molecules with high repeatability make these 2D arrays very attractive for SERS applications. Moreover, the geometry is fully consistent and compatible with the nano-imprinting lithography that could be employed to realize cheaper and affordable SERS substrates with very-high controllability and reproducibility.

Additionally, these 2D arrays may also be used contemporaneously for linear[18,19] and nonlinear characterization, where the detection of bio-molecules and/or warfare agents can be achieved by measuring, at the same time, the shift due to the variation of the refractive index and the Raman signal. This would boost the performances of actual devices devoted to sensing applications and their integration in microfluidic devices to combine all these capabilities with a real time SERS detection system. Finally, these 2D arrays establish a platform that may be easily integrated with graphene sheets in order to quench molecular fluorescence, improving the Raman SNR ratio and reducing unwanted background.[12]

The authors acknowledge the "Progetto Regione Puglia – Laboratorio Regionale di Sintesi e Caratterizzazione di Nuovi Materiali Organici e Nanostrutturati per Elettronica, Fotonica e Tecnologie Avanzate" from Regione Puglia. M.G. acknowledges partial financial support from the Army Research Office (W911NF-11-1-0284_1490-AM-01).

[1]P. L. Stiles, J. A. Dieringer, N. C. Shah, and R. P. Van Duyne, Annu. Rev. Anal. Chem. **1**, 601–626 (2008).
[2]H. Raether, *Surface Polaritons on Smooth and Rough Surfaces and on Gratings* (Springer-Verlag, Berlin, 1988).
[3]S. Maier, *Plasmonics: Fundamentals and Applications* (Springer, 2007).
[4]M. Muniz-Miranda, B. Pergolese, A. Bigotto, and A. Giusti, J. Colloid Interface Sci. **314**, 540–544 (2007).
[5]M. Cyrankiewicz, T. Wybranowski, and S. Kruszewski, J. Phys.: Conf. Ser. **79**, 012013 (2007).
[6]W. E. Doering and S. Nie, J. Phys. Chem. B **106**, 311–317 (2002).
[7]G. Bruno, G. V. Bianco, M. M. Giangregorio, A. Sacchetti, P. Capezzuto, and M. Losurdo, Appl. Phys. Lett. **96**, 043104 (2010).
[8]A. Merlen, V. Gadenne, J. Romann, V. Chevallier, L. Patrone, and J. C. Valmalette, Nanotechnology **20**, 215705 (2009).
[9]A. Lesuffleur, L. K. S. Kumar, A. G. Brolo, K. L. Kavanagh, and R. Gordon, J. Phys. Chem. C **111**, 2347–2350 (2007).
[10]F. Lordan, J. H. Rice, B. Jose, R. J. Forster, and T. E. Keyes, Appl. Phys. Lett. **99**, 033104 (2011).
[11]C. Y. Chan, J. B. Xu, M. Y. Waye, and H. C. Ong, Appl. Phys. Lett. **96**, 033104 (2010).
[12]Q. Hao, B. Wang, J. A. Bossard, B. Kiraly, Y. Zeng, I.-K. Chiang, L. Jensen, D. H. Werner, and T. J. Huang, J. Phys. Chem. C **116**, 7249–7254 (2012).
[13]Q. Hao, Y. Zeng, B. K. Juluri, X. Wang, B. Kiraly, I. Chiang, L. Jensen, D. H. Werner, V. H. Crespi, and T. J. Huang, ACS Nano **5**, 5472 (2011).
[14]D. de Ceglia, M. A. Vincenti, M. Scalora, N. Akozbek, and M. J. Bloemer, AIP Adv. **1**, 032151 (2011).
[15]M. Grande, R. Marani, F. Portincasa, G. Morea, V. Petruzzelli, A. D'Orazio, V. Marrocco, D. de Ceglia, and M. A. Vincenti, Sens. Actuators B **160**, 1056–1062 (2011).
[16]M. Scalora, M. A. Vincenti, D. de Ceglia, M. Grande, and J. W. Haus, "Raman scattering near metal nanostructures," J. Opt. Soc. Am. B **29**, 2035–2044 (2012).
[17]R. Marani, M. Grande, V. Marrocco, A. D'Orazio, V. Petruzzelli, M. A. Vincenti, and D. de Ceglia, Opt. Lett. **36**, 903–905 (2011).
[18]M. Grande, M. A. Vincenti, T. Stomeo, G. Morea, R. Marani, V. Marrocco, V. Petruzzelli, A. D'Orazio, R. Cingolani, M. De Vittorio, D. de Ceglia, and M. Scalora, Opt. Express **19**, 21385–21395 (2011).
[19]M. A. Vincenti, M. Grande, D. de Ceglia, T. Stomeo, V. Petruzzelli, M. De Vittorio, M. Scalora, and A. D'Orazio, Appl. Phys. Lett. **100**, 201107 (2012).
[20]G. Bruno, F. Babudri, A. Operamolla, G. V. Bianco, M. Losurdo, M. M. Giangregorio, O. H. Omar, F. Mavelli, G. M. Farinola, P. Capezzuto, and F. Naso, Langmuir **26**, 8430–8440 (2010).
[21]E. C. Le Ru, E. Blackie, M. Meyer, and P. G. Etchegoin, J. Phys. Chem. C **111**, 13794–13803 (2007).
[22]Y.-T. Tao, C.-C. Wu, J.-Y. Eu, W.-L. Lin, K.-C. Wu, and C.-H. Chen, Langmuir **13**, 4018–4023 (1997).
[23]C. Wang, Y. Chang, J. Yao, C. Luo, S. (Shizhuo) Yin, P. Ruffin, C. Brantley, and E. Edwards, Appl. Phys. Lett. **100**, 023107 (2012).
[24]C. Forestiere, Al. J. Pasquale, A. Capretti, G. Miano, A. Tamburrino, S. Y. Lee, B. M. Reinhard, and L. Dal Negro, Nano Lett. **12**, 2037–2044 (2012).